Estimating winter balance and its uncertainties from direct measurements of snow depth and density on alpine glaciers

Alexandra PULWICKI,[1] Gwenn E. FLOWERS,[1] Valentina RADIĆ,[2]

[1] *Department of Earth Sciences, Faculty of Science, Simon Fraser University, Burnaby, BC, Canada*

[2] *Department of Earth, Ocean and Atmospheric Sciences, Faculty of Science, University of British Columbia, Vancouver, BC, Canada*

Correspondence: Alexandra Pulwicki <apulwick@sfu.ca>

ABSTRACT. Accurately estimating winter surface mass balance on glaciers is central to assessing glacier health and predicting glacier runoff. However, measuring and modelling snow distribution is inherently difficult in mountainous terrain, resulting in high uncertainties in estimates of winter balance. In this study, we explore rigorous statistical methods of estimating winter balance and its uncertainty from direct measurements of snow depth and density at multiple scales. We collected more than 9000 direct measurements of snow depth across three glaciers in the St. Elias Mountains, Yukon, Canada in May 2016. Linear regression and simple kriging, combined with cross correlation and Bayesian model averaging, are used to interpolate point-scale winter balance estimates across the glacier. Elevation and a simple wind-redistribution parameter are found to be the dominant controls on the spatial distribution of winter balance, but the relationship varies considerably between glaciers. Through a Monte Carlo analysis, we find that the interpolation of winter balance values is a larger source of uncertainty than the assignment of snow density or than the subgrid variability. For our study glaciers, the

winter balance uncertainty from all assessed sources ranges from 0.03 m w.e. (8%) to 0.15 m w.e. (54%) depending primarily on the interpolation method. Despite the challenges associated with estimating winter balance, our results are consistent with a regional-scale winter-balance gradient. (220 words)

INTRODUCTION

Winter surface mass balance, or "winter balance", is the net accumulation and ablation of snow over the winter season (Cogley and others, 2011), which constitutes glacier mass input. Winter balance is half of the seasonally resolved mass balance, initializes summer ablation conditions, and ... (e.g. Hock, 2005; Réveillet and others, 2016). Effectively representing the spatial distribution of snow is also important for modelling energy and mass exchange between the land and atmosphere, allowing for better monitoring of surface runoff and its downstream effects (e.g. Clark and others, 2011).

Winter balance (WB) is notoriously difficult to estimate. Snow distribution in alpine regions is highly variable with short correlation length scales (e.g. Anderton and others, 2004; Egli and others, 2011; Grunewald and others, 2010; Helbig and van Herwijnen, 2017; López-Moreno and others, 2011, 2013; Machguth and others, 2006; Marshall and others, 2006) and is influenced by dynamic interactions between the atmosphere and complex topography, operating on multiple spatial and temporal scales (e.g. Barry, 1992; Liston and Elder, 2006; Clark and others, 2011). Simultaneously extensive, high resolution and accurate snow distribution measurements on glaciers are therefore almost impossible to obtain (e.g. Cogley and others, 2011; McGrath and others, 2015). Further, current models are computationally intensive and require extensive meteorological data to force the model (Dadić and others, 2010). As a result, there is significant uncertainty in estimates of winter balance and this limits the ability of models to represent current and projected glacier conditions.

Studies that have focused on obtaining detailed estimates of WB have used a wide range of observational techniques, including direct measurement of snow depth and density (e.g. Cullen and others, 2017), lidar or photogrammerty (e.g. Sold and others, 2013) and ground-penetrating radar (e.g. Machguth and others, 2006; Gusmeroli and others, 2014; McGrath and others, 2015). Spatial coverage of direct measurements is generally limited and often comprises an elevation transect along the glacier centreline (e.g. Kaser and others, 2002). Measurement are often interpolated using a linear regression on only a few topographic parameters (e.g. MacDougall and Flowers, 2011), with elevation being the most common. Other established techniques include hand contouring (e.g. Tangborn and others, 1975), kriging (e.g. Hock and Jensen, 1999) and attributing

measured winter balance values to elevation bands (e.g. Thibert and others, 2008). Physical snow models have been used to estimate spatial patterns of winter balance (e.g. Mott and others, 2008; Schuler and others, 2008; Dadić and others, 2010) but limited meteorological data generally prohibits their wide spread application. Error analysis is rarely undertaken and few studies have thoroughly investigated uncertainty in spatially distributed estimates of winter balance estimates (c.f. Schuler and others, 2008).

More sophisticated snow survey designs and statistical models of snow distribution are available and widely used in the field of snow science. Surveys described in the snow science literature are generally spatially extensive and designed to measure snow depth and density throughout a basin, ensuring that all terrain types are sampled. A wide array of measurement interpolation methods are used, including linear (e.g. López-Moreno and others, 2010) and non-linear regressions (e.g. Molotch and others, 2005) that include numerous terrain parameters, as well as geospatial interpolation (e.g. Erxleben and others, 2002) including various forms of kriging. Different interpolation methods are often combined (e.g. regression kriging) to yield improved fits (e.g. Balk and Elder, 2000). Physical snow models such as Alpine3D (Lehning and others, 2006) and SnowDrift3D (Schneiderbauer and Prokop, 2011) are widely used in snow science, and errors in estimating snow distribution have been examined from theoretical (e.g. Trujillo and Lehning, 2015) and applied perspectives (e.g. Turcan and Loijens, 1975; Woo and Marsh, 1978; Deems and Painter, 2006).

The goals of this study are to (1) critically examine methods of converting direct snow depth and density measurements to distributed estimates of winter balance and to (2) identify sources of uncertainty, evaluate their magnitude and assess their combined contribution to uncertainty in glacier-wide winter balance. We focus on commonly applied, low-complexity methods of measuring and estimating winter balance in the interest of making our results broadly applicable.

STUDY SITE

The St. Elias Mountains (Fig. 1a) rise sharply from the Pacific Ocean, creating a significant climatic gradient between coastal maritime conditions, generated by Aleutian–Gulf of Alaska low-pressure systems, and interior continental conditions, driven by the Yukon–Mackenzie high-pressure system (Taylor-Barge, 1969). The boundary between the two climatic zones is generally aligned with the divide between the Hubbard and Kaskawulsh Glaciers, approximately 130 km from the coast. The Donjek Range is located approximately 40 km to the east of this divide. Research on snow distribution and glacier mass balance in this area is limited. A series of research programs, including Project “Snow Cornice” and the Icefield Ranges Research Project,

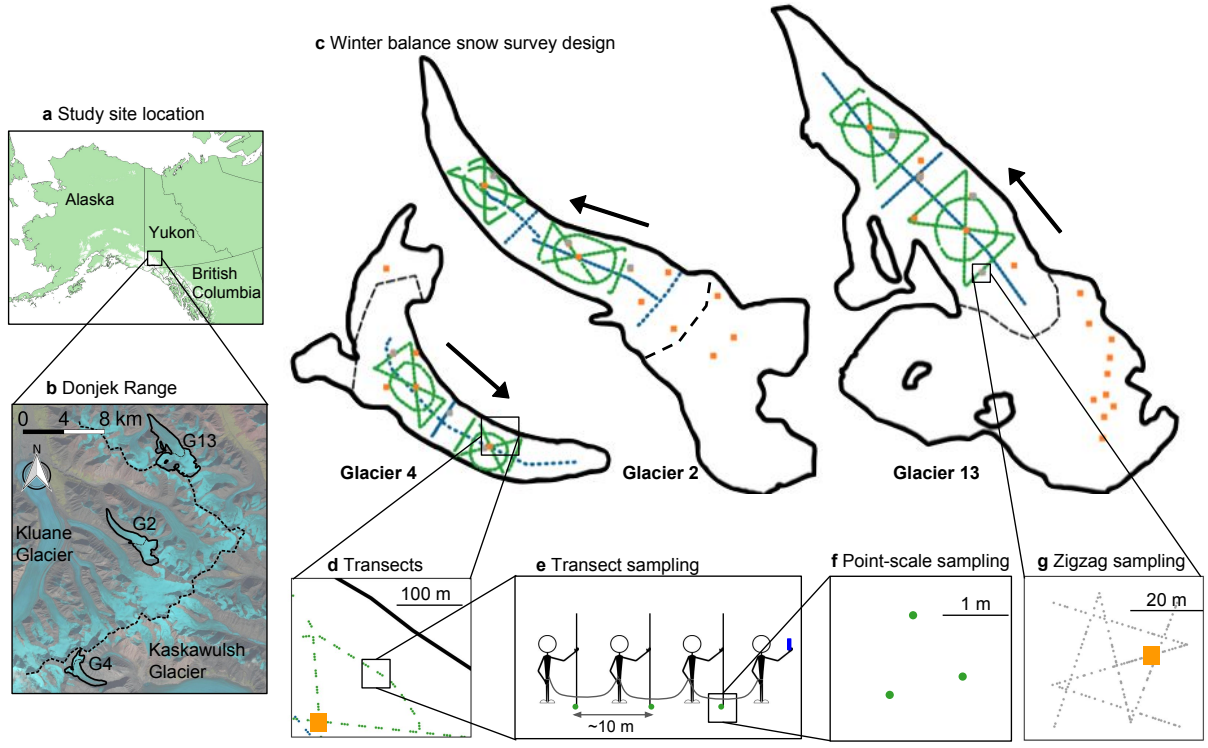

Fig. 1: Study area location and sampling design for Glaciers 4, 2 and 13. (a) Study region in the Donjek Range of the St. Elias Mountains of Yukon, Canada. (b) Study glaciers located along a southwest-northeast transect through the Donjek Range. The local topographic divide is shown as a dashed line. Imagery from Landsat8 (5 September 2013, data available from the U.S. Geological Survey). (c) Details of the snow-survey sampling design, with centreline and transverse transects (blue dots) and hourglass and circle designs (green dots) and locations of snow density measurements (orange squares). Arrows indicate glacier flow direction. Approximate location of ELA is shown as a black dashed line. (d) Close up of linear and curvilinear transects. (e) Configuration of observers. (f) Point-scale snow depth sampling.(g) Linear-random snow-depth measurements in 'zigzag' design (grey dots) with one density measurement (orange square) per zigzag.

were operational in the 1950s and 60s (Wood, 1948; Danby and others, 2003) and in the last 30 years, there have been a few long-term studies on select alpine glaciers (Clarke, 2014).

Winter balance surveys were conducted on three glaciers in the Donjek Range of the St. Elias Mountains. The Donjek Range is approximately 30 × 30 km and Glacier 4, Glacier 2 and Glacier 13 (labelling adopted from Crompton and Flowers (2016)) are located along a southwest-northeast transect through the range (Fig. 1b, Table 1). These small, polythermal alpine glaciers are generally oriented southeast-northwest, with Glacier 4 having a predominantly southeast facing aspect and Glaciers 2 and 13 have generally northwest facing aspects. The glaciers are situated in valleys with steep walls have simple geometries.

Table 1: Physical characteristics of study glaciers and May 2016 winter-balance survey details for study glaciers, including number of snow-depth measurement locations along transects (n_{T}), total length of transects (d_{T}), number of combined snow pit (SP) and Federal Sampler (FS) density measurement locations (n_{ρ}) and number of zigzag surveys (n_{zz}).

	Location	**Elevation (m a.s.l)**			**Slope (°)**	**Area**	**Survey**	**Survey Details**			
	UTM Zone 7	*Mean*	*Range*	*ELA*	*Mean*	**(km)**	**Dates**	n_{T}	d_{T} (km)	n_{ρ}	n_{zz}
Glacier 4	595470 E 6740730 N	2344	1958–2809	∼2500	12.8	3.8	4–7 May 2016	649	13.1	10	3
Glacier 2	601160 E 6753785 N	2495	1899–3103	∼2500	13.0	7.0	8–11 May 2016	762	13.6	11	3
Glacier 13	604602 E 6763400 N	2428	1923–3067	∼2380	13.4	12.6	12–15 May 2016	941	18.1	20	4

METHODS

Estimating glacier-wide WB involves transforming measurements of snow depth and density into distributed winter balance across a defined grid. We do this in four steps. (1) Obtain direct measurements of snow depth and density in the field. (2) Assign density values to all depth-measurement locations to calculate point-scale WB at each location. (3) Average all point-scale WB values within each gridcell of a digital elevation model (DEM) to obtain the gricell-averaged WB. (4) Interpolate and extrapolate these gridcell-averaged WB values to obtain estimates of WB (in m w.e.) in each gridcell across the domain. In Step 4, we use linear regression between gridcell-averaged WB and various topographic parameters because this method has precedent for success (e.g. McGrath and others, 2015). Instead of a basic regression, we use cross-validation and model averaging to test all combinations of the chosen topographic parameters.We compare the regression approach with simple kriging (SK), a data-driven interpolation method, to interpolate WB in Step 4 without invoking physical interpretation (e.g. Hock and Jensen, 1999). For brevity, we refer to these four steps as (1) field measurements, (2) density assignment, (3) gridcell-averaged WB and (4) distributed WB. Detailed methodology for each step is outlined below.

Field measurements

Sampling design

The snow surveys were designed to capture variability in snow depth at regional, basin, gridcell and point scales (Clark and others, 2011). To capture variability at the regional scale we chose three glaciers along the dominant precipitation gradient in the St. Elias Mountains, Yukon (Fig. 1) (Taylor-Barge, 1969). To account for basin-scale variability, snow depth was measured along linear and curvilinear transects on each glacier (Fig. 1c) with sample spacing of $10 - 60$ m (Fig. 1d). Sample spacing was constrained by protocols for safe glacier travel, while survey scope was constrained by the need to complete surveys on all three glaciers within the period of peak accumulation. We selected centreline and transverse transects as the most commonly used survey in winter balance studies (e.g. Kaser and others, 2002; Machguth and others, 2006) as well as an hourglass pattern with an inscribed circle, which allows for sampling in multiple directions and easy travel (personal communication from C. Parr, 2016). To capture variability at the grid scale, we densely sampled up to four gridcells on each glacier using a linear-random sampling design we term 'zigzag'. To capture point-scale variability, each observer made 3–4 depth measurements within ∼1 m of each other (Fig. 1e) at each transect measurement location. In total, we collected more than 9000 snow depth measurements throughout the study area (Table 1).

Snow depth: transects

Winter balance can be estimated as the product of snow depth and depth-averaged density. Snow depth is generally accepted to be more variable than density (Elder and others, 1991; Clark and others, 2011; López-Moreno and others, 2013) so we chose a sampling design that resulted in a high ratio (∼55:1) snow depth to density measurements. Our sampling campaign involved four people and occurred between 5–15 May 2016, corresponding to the peak seasonal snow accumulation in Yukon (Yukon Snow Survey Bulletin and Water Supply Forecast, May 1, 2016). While roped-up for glacier travel at fixed distances between observers, the lead observer used a single-frequency GPS unit (Garmin GPSMAP 64s) to navigate between predefined transect measurement locations (Fig. 1e). The remaining three observers used 3.2 m graduated aluminium avalanche probes to make snow depth measurements. The locations of each set of depth measurements, made by the second, third and fourth observers, are estimated using the recorded location of the first observer, the known distance between observers and the direction of travel.

Snow-depth sampling was concentrated in the ablation area to ensure that only snow from the current accumulation season was measured. The boundary between snow and firn in the accumulation area can be

difficult to detect and often misinterpreted, especially when using an avalanche probe (Grunewald and others, 2010; Sold and others, 2013). We intended to use a firn corer to measure winter balance in the accumulation area, but cold snow combined with positive air temperatures led to cores being unrecoverable. Successful snow depth and density measurements within the accumulation area were made either in snow pits or using a Federal Sampler to unambiguously identify the snow–firn transition.

Snow depth: zigzags

To capture snow-depth variability within a single DEM gridcell, we implemented a linear-random zigzag sampling design (Shea and Jamieson, 2010). We measured depth at random intervals of 0.3–3.0 m along two 'Z'-shaped patterns, resulting in 135–191 measurements, within three to four 40×40 m gridcells (Fig. 1g) per glacier. Random intervals had a uniform distribution and were generated in MATLAB. Zigzag locations were randomly chosen within the upper, middle, and lower regions of the ablation area of each glacier. We were able to measure a fourth zigzag on Glacier 13 that was located in the central ablation area, ~2200 m a.s.l.

Snow density

Snow density was measured using a Snowmetrics wedge cutter in three snow pits on each glacier, as well as with a Geo Scientific Ltd. metric Federal Sampler. Within the snow pits (SP), we measured a vertical density profile (at 5 cm increments) with the $5 \times 10 \times 10$ cm wedge-shaped cutter (250 cm^3) and a Presola 1000 g spring scale (e.g. Gray and Male, 1981; Fierz and others, 2009). Uncertainty in estimating density from snow pit measurements stems from incorrect assignment of density to layers that cannot be sampled (e.g. ice lenses and hard layers). We attempt to quantify this uncertainty by varying estimated ice layer thickness by ± 1 cm ($\leq$100%) of the recorded thickness, ice layer density between 700 and 900 $kg\,m^{-3}$ and the density of layers identified as being too hard to sample (but not ice) between 600 and 700 $kg\,m^{-3}$. When considering all three sources of uncertainty, the range of integrated density values is always less than 15% of the reference density. Depth-averaged densities for shallow pits (<50 cm) that contain ice lenses are particularly sensitive to changes in prescribed density and ice-lens thicknesses.

While snow pits provide the most accurate measure of snow density, digging and sampling a snow pit is time and labour intensive. Therefore, a Federal Snow Sampler (FS) (Clyde, 1932), which directly measures depth-integrated snow-water equivalent, was used to augment the snow pit measurements. A minimum of three Federal Sampler measurements were taken at each of $7-19$ locations on each glacier and an additional eight Federal Sampler measurements were co-located with each snow pit profile. Measurements for which

the snow core length inside the sampling tube was less than 90% of the snow depth were discarded. Density values at each measurement location (eight at snow pit locations, three elsewhere) were then averaged to obtain the uncertainty, which is taken to be the standard deviation of these measurements.

During the field campaign there were two small accumulation events. The first, on 6 May 2016, also involved high winds so accumulation could not be determined. The second, on 10 May 2016, resulted in 0.01 m w.e accumulation measured at one location on Glacier 2. Positive temperatures and clear skies occurred between 11–16 May 2016, which we suspect resulted in melt occurring on Glacier 13. The snow in the lower part of the ablation area of Glacier 13 was isothermal and showed clear signs of melt and metamorphosis. The total amount of accumulation and melt during the study period could not be estimated so no corrections were made.

Density assignment

Measured snow density must be interpolated or extrapolated to estimate point-scale winter balance at each snow-depth sampling location. We employ four commonly used methods to interpolate and extrapolate density (Table 2): (1) calculate mean density over an entire mountain range (e.g. Cullen and others, 2017), (2) calculate mean density for each glacier (e.g. Elder and others, 1991; McGrath and others, 2015), (3) linear regression of density on elevation for each glacier (e.g. Elder and others, 1998; Molotch and others, 2005) and (4) calculate mean density using inverse-distance weighting (e.g. Molotch and others, 2005) for each glacier. SP- and FS-derived densities are treated separately, for reasons explained below, resulting in eight possible methods of assigning density.

Gridcell-averaged winter balance

We average one to six (mean of 2.1 measurements) point-scale values of WB within each 40×40 m DEM gridcell to obtain the gricell-averaged WB. The locations of individual measurements have uncertainty due to the error in the horizontal position given by the GPS unit and the estimation of observer location based on the recorded GPS positions of the navigator. This location uncertainty could result in the incorrect assignment of a point-scale WB to a particular gridcell. However, this source of error is not further investigated because we assume that the uncertainty in gridcell-averaged WB is captured in the zigzag measurements described below. Uncertainty due to having multiple observers was also tested. There are no significant differences between snow depth measurements made by observers along a transect ($p>0.05$), with the exception of the first transect on Glacier 4 (51 measurements).

Table 2: Eight methods used to estimate snow density at unmeasured locations for purpose of converting measured snow depth to point-scale winter balance.

Method code	Source of measured snow density		Density assignment method
	Snow pit	*Federal Sampler*	
S1	■		Mean of measurements
F1		■	across all glaciers
S2	■		Mean of measurements
F2		■	within a given glacier
S3	■		Regression of density on
F3		■	elevation within a glacier
S4	■		Inverse distance
F4		■	weighted mean

Distributed winter balance

Linear regression

Gridcell-averaged values of WB are interpolated and extrapolated across each glacier using linear regression (LR) and simple kriging (SK). The regression relates gridcell-averaged values of WB to DEM-derived topographic parameters. We use commonly applied topographic parameters as in McGrath and others (2015), including elevation, slope, aspect, curvature, "northness" and a wind-redistribution parameter; we add distance-from-centreline as an additional parameter. Our sampling design ensured that the ranges of topographic parameters associated with our measurement locations represent more than 70% of the total area of each glacier (except elevation on Glacier 2, where our measurements captured only 50%). Topographic parameters are standardized and then weighted by a set of fitted regression coefficients (β_i) calculated by minimizing the sum of squares of the vertical deviations of each datum from the regression line (Davis and Sampson, 1986). For details on data and methods used to estimate the topographic parameters see the Supplementary Material.

To avoid overfitting the data and to incorporate every possible combination of topographic parameters, cross-validation and model averaging are implemented. First, cross-validation is used to obtain a set of β_i values that have the greatest predictive ability. We randomly select 1000 subsets of the data (2/3 of the

values) to fit the LR and use the remaining data (1/3 of the values) to calculate a root mean squared error (RMSE) (Kohavi and others, 1995). Regression coefficients resulting in the lowest RMSE (1000 values) are selected. Second, we use model averaging to account for uncertainty when selecting predictors and to maximize the model's predictive ability (Madigan and Raftery, 1994). Models are generated by calculating a set of β_i for all possible combinations of topographic parameters (2^7 models). Following a Bayesian framework, model averaging involves weighting all models by their posterior model probabilities (Raftery and others, 1997). To obtain the final regression coefficients, the β_i values from each model are weighted according to the relative predictive success of the model, as assessed by the value of the Bayesian Information Criterion (BIC) (Burnham and Anderson, 2004). BIC penalizes more complex models which further reduces the risk of overfitting. The distributed WB is then obtained by applying the resulting regression coefficients to the topographic parameters associated with each gridcell.

Simple kriging

Simple kriging (SK) is a data-driven method of estimating variables at unsampled locations by using the isotropic spatial correlation (covariance) of measured values to find a set of optimal weights (Davis and Sampson, 1986; Li and Heap, 2008). Simple kriging assumes spatial correlation between sampling locations that are distributed across a surface and then applies the correlation to interpolate between these locations. We used the `DiceKriging` R package (Roustant and others, 2012) to calculate the maximum likelihood covariance matrix, as well as the range distance (θ) and nugget for gridcell-averaged values of winter balance. The range distance is a measure of data correlation length and the nugget is the residual that encompasses sampling-error variance as well as the spatial variance at distances less than the minimum sample spacing (Li and Heap, 2008). Unlike the topographic regression, simple kriging is not useful for generating hypotheses used to explore physical processes that may be controlling snow distribution and cannot be used to estimate winter balance on an unmeasured, neighbouring glacier.

Uncertainty analysis

To quantify the uncertainty on estimates of glacier-wide WB, we conduct a Monte Carlo analysis, which uses repeated random sampling of input variables to calculate a distribution of output variables (Metropolis and Ulam, 1949). We repeat the random sampling process 1000 times, resulting in a distribution of values of the glacier-wide WB based on uncertainties associated with the four steps outlined above. We use the standard deviation of this distribution as a useful metric on uncertainty of the glacier-wide WB. Three sources of uncertainty are considered separately: the uncertainty due to (1) variability of WB values at the grid-scale

(σ_{GS}), (2) the assignment of snow density (σ_{ρ}) and (3) interpolating and extrapolating gridcell-averaged values of WB (σ_{INT}). These individual sources of uncertainty are propagated through the conversion of snow depth and density measurements to glacier-wide winter balance. Finally, the combined effect of all three sources of uncertainty on the glacier-wide WB is quantified.

Grid-scale uncertainty (σ_{GS})

We make use of the grid-scale zigzag surveys to represent the true variability of WB at the grid scale. Our data do not permit a spatially-resolved assessment of grid-scale uncertainty so we assume the same grid-scale uncertainty between gridcells for each glacier and represent this uncertainty by a normal distribution. The normal distribution is centred at zero and has a standard deviation equal to the mean standard deviation of all zigzags on each glacier. For each iteration of the Monte Carlo, WB values are randomly chosen from the distribution and added to the values of gridcell-averaged WB. These perturbed gridcell-averaged values of WB are then used in the interpolation. We represent uncertainty in glacier-wide WB due to grid-scale uncertainty (σ_{GS}) as the standard deviation of the resulting distribution of glacier-wide WB estimates.

Density assignment uncertainty (σ_{ρ})

We incorporate uncertainty due to the method of density assignment by carrying forward all eight density interpolation methods (Table 2) when estimating glacier-wide WB. Using this arrangement of density interpolation methods results in a generous estimate of density assignment uncertainty. We represent the glacier-wide WB uncertainty due to density assignment uncertainty (σ_{ρ}) as the standard deviation of glacier-wide WB estimates calculated using each density assignment method.

Interpolation uncertainty (σ_{INT})

We represent the uncertainty due to interpolation of gridcell-averaged WB in different ways for LR and SK. LR interpolation uncertainty is represented by a multivariate normal distribution of possible regression coefficients (β_i). The standard deviation of each distribution is calculated using the covariance of regression coefficients as outlined in Bagos and Adam (2015), which ensures that regression coefficients are internally consistent. The β_i distributions are randomly sampled and used to calculate gridcell-estimated WB.

SK interpolation uncertainty is represented by the 95% confidence interval for gridcell-estimated values of WB generated by the `DiceKriging` package. From this confidence interval, the standard deviation of each gridcell-estimated WB is then calculated. The standard deviation of glacier-wide WB is then found by taking the square root of the average variance of each gridcell-estimated WB. The final distribution of

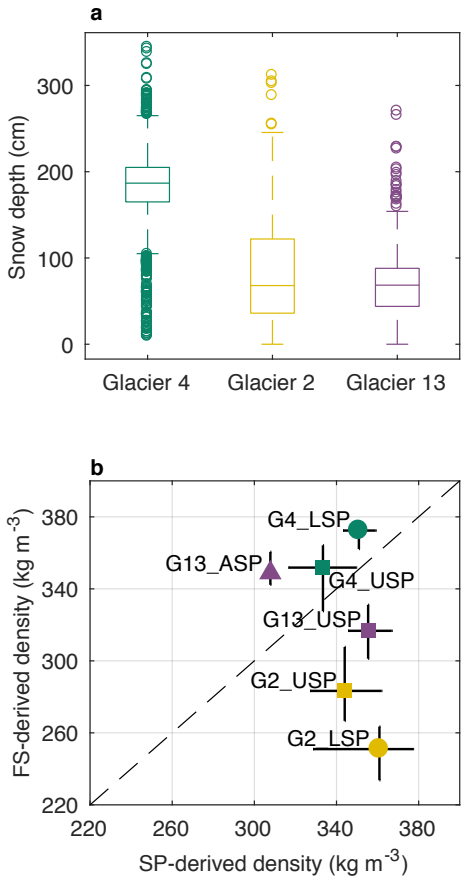

Fig. 2: Measured snow depth and density. (a) Boxplot of measured snow depth on Glaciers 4, 2 and 13 with the first quartiles (box), median (line within box), minimum and maximum values excluding outliers (bar) and outliers (circles), which are defined as being outside of the range of 1.5 times the quartiles (approximately $\pm 2.7\sigma$). (b) Comparison of depth-averaged densities estimated using Federal Sampler measurements (FS) and using a wedge cutter in a snow pit (SP) estimated for Glacier 4 (G4), Glacier 2 (G2) and Glacier 13 (G13). Labels indicate snow pit locations in the accumulation area (ASP), upper ablation area (USP) and lower ablation area (LSP). Error bars for SP-derived densities are calculated by varying the thickness and density of layers that are too hard to sample and error bars for FS-derived densities are the standard deviation of measurements taken at one location. One-to-one line is dashed.

glacier-wide WB values is centred at the SK glacier-wide WB estimate. For simplicity, the standard deviation of glacier-wide WB values that result from either LR or SK interpolation uncertainty is referred to as σ_{INT}.

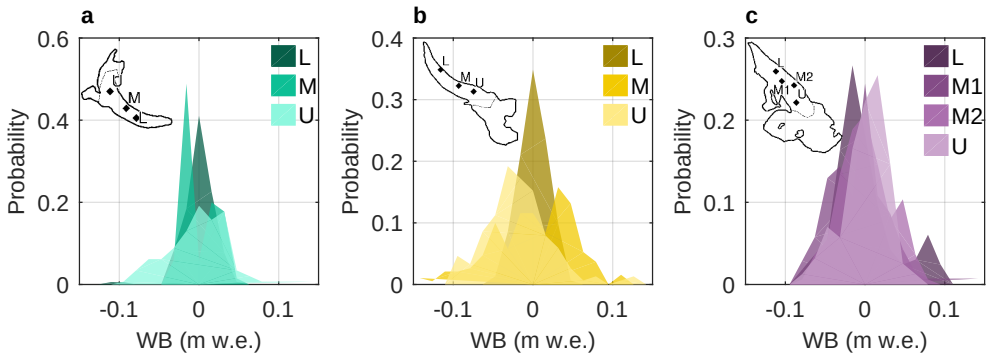

Fig. 3: Distributions of estimated winter balance values for each zigzag survey in lower (L), middle (M) and upper (U) ablation areas (insets). Local mean has been subtracted. (a) Glacier 4. (b) Glacier 2. (c) Glacier 13.

RESULTS AND DISCUSSION

Field measurements

Snow depth

Mean snow depth varied systematically across the study region, with Glacier 4 having the highest mean snow depth and Glacier 13 having the lowest (Fig. 2). At each measurement location, the median range of measured depths ($3-4$ points) as a percent of the mean local depth is 2%, 11% and 12%, for Glaciers 4, 2 and 13, respectively. While Glacier 4 has the lowest point-scale variability, as assessed above, it also has the highest proportion of outliers, indicating a more variable snow depth across the glacier. The average standard deviation of all zigzag depth measurements is 0.07 m, 0.17 m. and 0.14 m, for Glaciers 4, 2 and 13, respectively. When converted to values of winter using the local FS-derived density measurement, the average standard deviation is 0.027 m w.e., 0.035 m w.e. and 0.040 m w.e. WB data for each zigzag are not normally distributed about the mean WB value (Fig. 3).

Snow density

Contrary to expectation, co-located FS and SP measurements are found to be uncorrelated ($R^2 = 0.25$, Fig. 2b). The Federal Sampler appears to oversample in deep snow and undersample in shallow snow. Oversampling by small- diameter (3.2–3.8 cm) sampling tubes has been observed in previous studies, with a percent error between 6.8% and 11.8% (e.g. Work and others, 1965; Fames and others, 1982; Conger and McClung, 2009). Studies that use Federal Samplers often apply a 10% correction to all measurements for

this reason (e.g. Molotch and others, 2005). Oversampling has been attributed to slots "shaving" snow into the tube as it is rotated (e.g. Dixon and Boon, 2012) and to snow falling into the slots, particularly for snow samples with densities >400 kg m^{-3} and snow depths >1 m (e.g. Beauont and Work, 1963). Undersampling is likely to occur due to loss of snow from the bottom of the sampler (Turcan and Loijens, 1975). Loss by this mechanism may have occurred in our study given the isothermal and melt-affected snow conditions observed over the lower reaches of Glaciers 2 and 13. Relatively poor Federal Sampler spring-scale sensitivity also calls into question the reliability of measurements for snow depths <20 cm.

We also found that Federal Sampler density values are positively correlated with snow depth ($R^2 = 0.59$). This positive relationship could be a result of physical processes, such as compaction in deep snow and preferential formation of depth hoar in shallow snow, but is more likely a result of measurement artefacts for a number of reasons. First, the range of densities measured by the Federal Sampler is large (227–431 kg m^{-3}) and the extreme values seem unlikely given the conditions at the time of sampling. Second, compaction effects of the magnitude required to explain the density differences between snow pit and Federal Sampler measurements would not be expected at the measured snow depths (up to 340 cm). Third, no linear relationship exists between depth and SP-derived density ($R^2 = 0.05$). These findings indicate that the Federal Sampler measurements have a bias which we have not identified a suitable correction.

Density assignment

Given the lack of correlation between co-located SP- and FS-derived densities (Fig. 2), we use the densities derived from these two methods separately (Table 2). SP-derived regional (S1) and glacier-mean (S2) densities are within one standard deviation of the corresponding FS-derived densities (F1 and F2) although SP-derived density values are larger (see Supplementary Material, Table S2). For both SP- and FS-derived densities, the mean density for any given glacier (S2 or F2) is within one standard deviation of the mean across all glaciers (S1 or F1). Correlations between elevation and SP- and FS-derived densities are generally high ($R^2 > 0.5$) but vary between glaciers (Supplementary material, Table S2). For any given glacier, the standard deviation of the 3–4 SP- or FS-derived densities is <13% of the mean of those values (S2 or F2) (Supplementary material, Table **??**). We adopt S2 (glacier-wide mean of SP-derived densities) as the reference method of density assignment. Though the method described by S2 does not account for known basin-scale spatial variability in snow density (e.g. Wetlaufer and others, 2016), it is consistent with most winter balance studies, which assume a uniform density for individual glaciers and measure snow density profiles at multiple locations in a study basin (e.g. Elder and others, 1991; McGrath and others, 2015; Cullen and others, 2017).

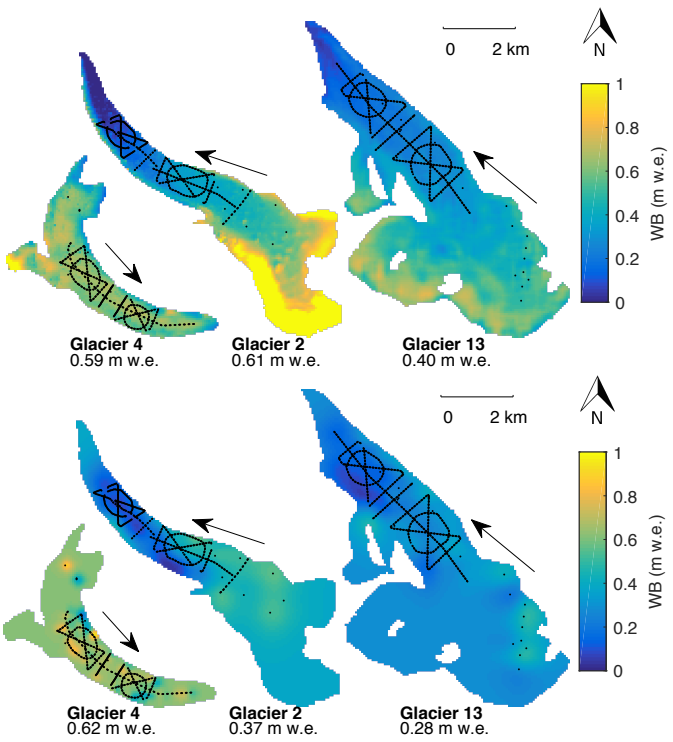

Fig. 4: Spatial distribution of winter balance (WB) estimated using linear regression (top row) and simple kriging (bottom row) with densities assigned as per S2 (Table 2). Locations of snow depth measurements are shown as black dots. Glacier flow directions are indicated by arrows. Values of glacier-wide WB are given below labels.

Gridcell-averaged winter balance

The distributions of gridcell-averaged WB values for the individual glaciers are similar to those in Fig. 2a but with fewer outliers. The standard deviation of WB values determined from the zigzag surveys are almost twice as large as the mean standard deviation of point-scale WB values within a gridcell measured along transects. However, a small number of gridcells sampled in transect surveys have standard deviations in WB that exceed 0.25 m w.e. (∼10 times greater than zigzag standard deviations). We nevertheless assume that the gridcell uncertainty is captured with dense sampling in zigzag gridcells.

Distributed winter balance

Linear Regression

Of the topographic parameters in the linear regression, elevation (z) is the most significant predictor of gridcell-averaged WB for Glaciers 2 and 13, while wind redistribution (Sx) is the most significant predictor for Glacier 4 (Fig. 5). As expected, gridcell-averaged WB is positively correlated with elevation where the

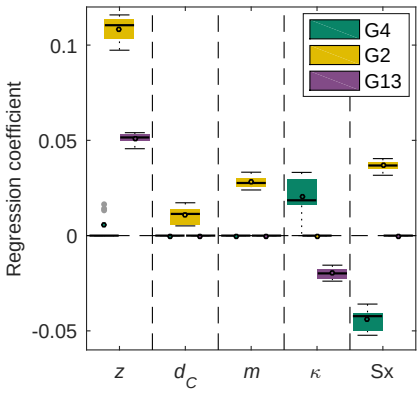

Fig. 5: Distribution of coefficients (β_i) determined by linear regression of gridcell-averaged WB on DEM-derived topographic parameters for the eight different density assignment methods (Table 2). Coefficients are calculated using standardized data, so values can be compared across parameters. Regression coefficients that are not significant are assigned a value of zero. Topographic parameters include elevation (z), distance from centreline (d_C), slope (m), curvature (κ) and wind redistribution (Sx). Aspect (α) and "northness" (N) are not shown because coefficient values are zero in every case. The box plot shows first quartiles (box), median (line within box), mean, (circle within box), minimum and maximum values excluding outliers (bar) and outliers (gray dots), which are defined as being outside of the range of 1.5 times the quartiles (approximately $\pm 2.7\sigma$).

correlation is significant. It is possible that the elevation correlation was accentuated due to melt onset for Glacier 13 in particular. In our study, the dependence of WB on elevation results in ∼1% of the area of Glacier 2 with gridcell-estimated WB >1.5 m w.e. Many winter balance studies have found elevation to be the most significant predictor of winter balance data (e.g. Machguth and others, 2006; McGrath and others, 2015). However, WB–elevation gradients vary considerably between glaciers (e.g. Winther and others, 1998) and other factors, such as glacier orientation relative to dominant wind direction and glacier shape, are strong predictors of winter balance distribution (Machguth and others, 2006; Grabiec and others, 2011). Some studies that find no significant correlation between WB on glaciers and topographic parameters, with highly variable distributions of snow attributed to complex interactions between topography and the atmosphere that could not be easily quantified (e.g. Grabiec and others, 2011; López-Moreno and others, 2011). Extrapolating relationships to unmeasured locations, especially the accumulation area, is susceptible to large uncertainties

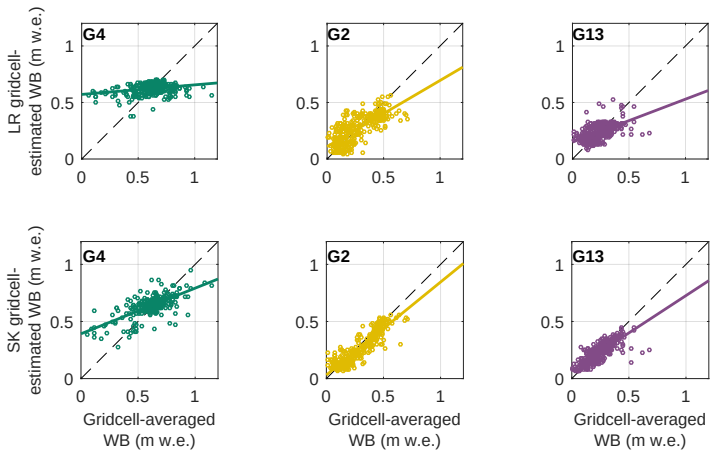

Fig. 6: Winter balance (WB) estimated by linear regression (LR, top row) or simple kriging (SK, bottom row) versus the grid-cell averaged WB data for Glacier 4 (left), Glacier 2 (middle) and Glacier 13 (right). Each circle represents a single gridcell. Best-fit (solid) and one-to-one (dashed) lines are shown.

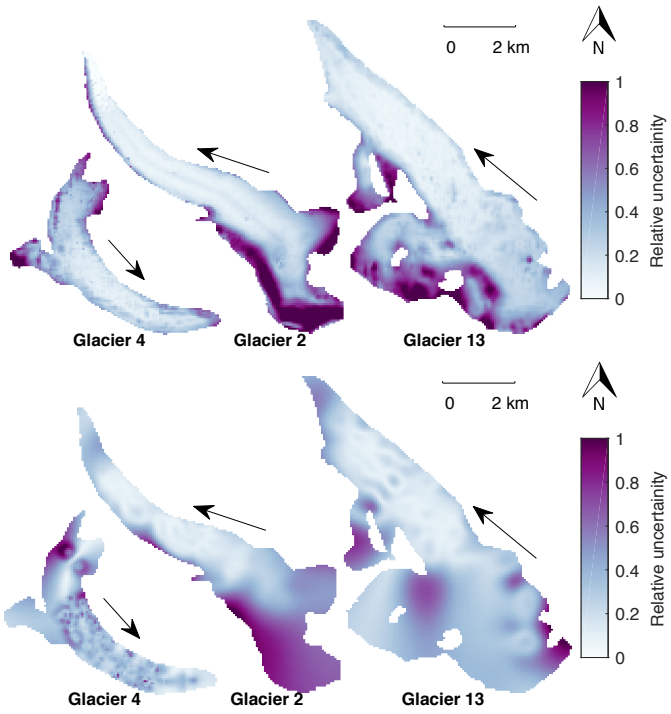

Fig. 7: Relative uncertainty in distributed winter balance (WB) (Fig. 4) found using linear regression (top row) and simple kriging (bottom row). Relative uncertainty is calculated as the sum of differences between every pair of one hundred estimates of gridcell-estimated WB that include grid-scale and interpolation uncertainty. The sum is then normalized for each glacier. Values closer to one indicate higher relative uncertainty. Glacier flow directions are indicated by arrows.

Table 3: Glacier-wide winter balance (WB, m w.e.) estimated using linear regression and simple kriging for the three study glaciers. Root mean squared error (RMSE, m w.e.) is computed as the average of all RMSE values between gridcell-averaged values of WB (the data) that were randomly selected and excluded from interpolation (1/3 of all data) and those estimated by interpolation. RMSE as a percent of the glacier-wide WB is shown in brackets.

	Linear regression		**Simple kriging**	
	WB	RMSE	WB	RMSE
G4	0.58	0.15 (26%)	0.62	0.13 (21%)
G2	0.58	0.10 (17%)	0.37	0.07 (19%)
G13	0.38	0.08 (21%)	0.27	0.07 (26%)

(Fig. 7). This extrapolation has a considerable effect on the glacier-wide WB values because the accumulation area typically has the largest values of winter balance (Fig. 4).

Gridcell-averaged WB is negatively correlated with Sx on Glacier 4, counter-intuitively indicating less snow in what would be interpreted as sheltered areas. Gridcell-averaged WB is positively correlated with Sx on Glaciers 2 and 13. Similarly, gridcell-averaged WB is positively correlated with curvature on Glacier 4 and negatively correlated on Glaciers 2 and 13. Wind redistribution and preferential deposition of snow are known to have a large influence on accumulation at sub-basin scales (e.g. Dadić and others, 2010; Winstral and others, 2013; Gerber and others, 2017). Our results point to wind having an impact on snow distribution, but the wind redistribution parameter (Sx) may not adequately capture these effects at our study glaciers. For example, Glacier 4 is located in a curved valley with steep side walls, so specifying a single cardinal direction for wind may not be adequate. Further, the scale of deposition may be smaller than the resolution of the Sx parameter estimated from our DEM. Our results corroborate those of McGrath and others (2015), in a study of six glaciers in Alaska (DEM resolutions of 5 m) where elevation and Sx were the only significant parameters for all glaciers; Sx regression coefficients were smaller than elevation regression coefficients, and in some cases, negative. Sublimation from blowing snow has also been shown to be an important mechanism mass loss from ridges (e.g. Musselman and others, 2015). Incorporating such losses, as well as redistribution and preferential deposition, may be important for improving representations of distributed winter balance.

While LR has been used to predict winter balance in unmeasured basins, we find that transfer of LR coefficients between glaciers results in large estimation errors. Regression coefficients from Glacier 4 produce the highest root mean squared error for all three glaciers (0.31 m w.e.) and glacier-wide WB values are

equivalent (0.64 m w.e.). Even when WB values for all three glaciers are combined, root mean squared error is large (0.20 m w.e.). Our results are consistent with Grünewald and others (2013), who found that local statistical models cannot be transferred across basins and that regional-scale models are not able to explain the majority of observed variance in winter balance.

Simple kriging

Fitted kriging parameters, including the nugget and spatial correlation length, can provide insight into important scales of winter balance variability. The model fitted to the gridcell-averaged values of WB for Glacier 4 has a short correlation length (90 m) and large nugget (see Supplementary Material Table S3), indicating that accumulation variability occurs at smaller scales. Conversely, Glaciers 2 and 13 have longer correlation lengths (∼450 m) and smaller nuggets, indicating variability at larger scales. Additionally, simple kriging is better able to estimate values of WB for Glaciers 2 and 13 than for Glacier 4 (Figure 6). Simple kriging produces almost uniform gridcell-estimated values of winter balance in the accumulation area of each glacier, which is inconsistent with observations described in the literature (e.g. Machguth and others, 2006; Grabiec and others, 2011). Extrapolation using simple kriging leads to large uncertainty (Fig. 7), further emphasizing the need for spatially distributed point-scale measurements.

LR and SK comparison

Glacier-wide WB estimates found using both LR and SK are ∼0.58 m w.e. for Glacier 4 but both are poor predictors of WB in measured gridcells (Table 3). For Glaciers 2 and 13, SK estimates are more than 0.1 m w.e. (up to 40%) lower than LR estimates (Table 3). RMSE as a percentage of the glacier-wide WB are comparable between LR and SK (Table 3) with an average RMSE of 22%. Gridcell-estimated values of WB found using LR and SK differ markedly in the upper accumulation areas of Glaciers 2 and 13 (Fig. 4), where observations are sparse and topographic parameters, such as elevation, vary considerably. The influence of elevation results in substantially higher LR-estimated WBs at high elevation, whereas SK-estimated values approximate the nearest data. Estimates of ablation-area-wide WB differ by <7% between LR and SK on each glacier, further emphasizing that the choice of interpolation method affects how WB data are extrapolated, which has a large effect on glacier-wide WB estimates on our study glaciers.

Uncertainty analysis

Glacier-wide winter balance is affected by uncertainty introduced when by the representativeness of gridcell-averaged values of WB (σ_{GS}), choosing a method of density assignment (σ_{ρ}), and interpolating WB values

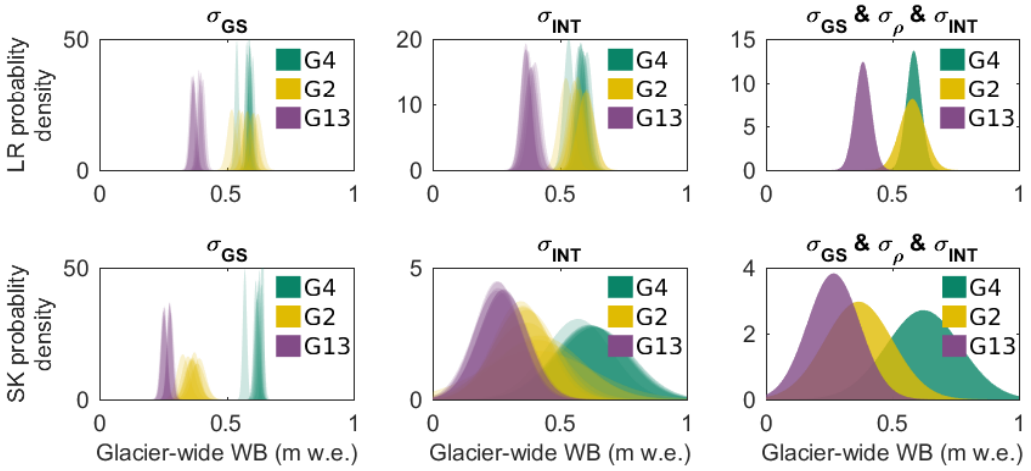

Fig. 8: Distributions of glacier-wide winter balance (WB) for Glaciers 4 (G4), 2 (G2) and 13 (G13) that arise from various sources of uncertainty. WB distribution arising from grid-scale uncertainty (σ_{GS}) (left column). WB distribution arising from interpolation uncertainty (σ_{INT}) (middle column). WB distribution arising from a combination of σ_{GS}, σ_{INT} and density assignment uncertainty (σ_{ρ}) (right column). Results are shown for interpolation by linear regression (LR, top row) and simple kriging (SK, bottom row). Left two columns include eight distributions per glacier (colour) and each corresponds to a density assignment method (S1–S4 and F1–F4).

across the domain (σ_{INT}). Using a Monte Carlo analysis, we find that σ_{INT} contributes more to WB uncertainty than σ_{GS} or σ_{ρ}. In other words, the distribution of glacier-wide WBs that arises from σ_{GS} and the differences in distributions between methods of density assignment are much smaller than the distribution that arises from σ_{INT} (Fig. 8 and Table 4). The WB distributions obtained using LR and SK overlap for a given glacier, but the distribution modes differ (Fig. 8). For reasons outlined above, SK-estimated values of WB in the accumulation area are generally lower, which lowers the glacier-wide WB estimate. The uncertainty in SK-estimated values of WB is large, and unrealistic glacier-wide values of WB of 0 m w.e. can be estimated (Fig. 8). Our results caution strongly against including extrapolated values of WB estimates from remote sensing or modelling studies because this may produce misleading results. If possible, such comparison should use point-scale data rather than interpolated values.

Grid-scale uncertainty (σ_{GS}) is the smallest assessed contributor to overall WB uncertainty. This result is consistent with generally smoothly-varying snow depth in zigzags and previously reported ice-roughness length on the order of centimetres (e.g. Hock, 2005). Given our assumption that zigzags are an accurate

representation of gridscale-variablity, low WB uncertainty arising from σ_{GS} implies that obtaining the most accurate value of gridcell-averaged WB does not need to be a priority when designing a snow survey. Our assumption that the 3–4 zigzag surveys can be used to estimate glacier wide σ_{GS} may not be true, particularly in areas with debris cover, crevasses and steep slopes.

Our uncertainty analysis did not include uncertainty arising from a number of sources, which we assume either to be encompassed by the sources investigated or to contribute negligibly to overall uncertainty. These sources of uncertainty include density measurement errors associated with wedge cutters, spring scales and depth measurement in snow pits and when using the Federal Sampler, vertical and horizontal error in the DEM as well as error associated with estimating measurement locations.

The values of glacier-wide WB of our three study glaciers (using S2 density assignment method), with an uncertainty equal to one standard deviation of the distribution found with Monte Carlo analysis, are: 0.59 ± 0.03 m w.e. on Glacier 4, 0.61 ± 0.05 m w.e. on Glacier 2 and 0.40 ± 0.03 m w.e. on Glacier 13.

Context and caveats

Regional winter-balance gradient

Although we find considerable inter- and intra-basin variability in winter balance, our results are consistent with a regional-scale WB gradient for the continental side of the St. Elias Mountains (Fig. 9). WB data are compiled from Taylor-Barge (1969), the three glaciers presented in this paper and two snow pits we analysed near the head of the Kaskawulsh Glacier between 20–21 May 2016. The data show a linear decrease of -0.024 m w.e. km^{-1} (R^2 =0.85) in winter balance with distance from the regional topographic divide between the Kaskawulsh and Hubbard Glaciers, as identified by Taylor-Barge (1969). While the three study glaciers fit the regional trend, the same relationship would not apply if just the Donjek Range were considered.

Table 4: Standard deviation ($\times 10^{-2}$ m w.e.) of glacier-wide winter balance distributions arising from uncertainties in grid-scale WB (σ_{GS}), density assignment (σ_ρ), interpolation (σ_{INT}) and all three sources combined (σ_{ALL}) for linear regression (left columns) and simple kriging (right columns)

	Linear regression				**Simple kriging**			
	σ_{GS}	σ_ρ	σ_{INT}	σ_{ALL}	σ_{GS}	σ_ρ	σ_{INT}	σ_{ALL}
Glacier 4	0.86	1.90	2.13	2.90	0.85	2.15	14.05	14.72
Glacier 2	1.80	3.37	3.09	4.90	2.53	2.03	13.78	13.44
Glacier 13	1.12	1.68	2.80	3.20	1.15	1.27	9.65	10.43

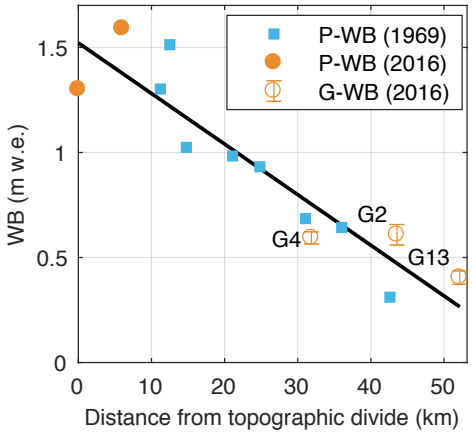

Fig. 9: Relationship between winter balance (WB) and linear distance from the regional topographic divide between the Kaskawulsh and Hubbard Glaciers in the St. Elias Mountains. Point-scale values of WB from snow-pit data reported by Taylor-Barge (1969) (blue boxes). LR-estimated glacier-wide WB calculated using density assignment S2 for Glaciers 4 (G4), 2 (G2) and 13 (G13) with errors bars calculated as the standard deviation of Monte Carlo-derived WB distributions (this study) (open orange circles). Point-scale WB estimated from snow-pit data at two locations in the accumulation area of the Kaskawulsh Glacier, collected in May 2016 (unpublished data, SFU Glaciology Group) (filled orange dots). Black line indicates best fit ($R^2 = 0.85$).

We hypothesize that interaction between meso-scale weather patterns and large-scale mountain topography is a major driver of regional-scale winter balance. Further insight into regional-scale patterns of winter balance can be gained by investigating moisture source trajectories and the contribution of orographic precipitation to winter balance across the St. Elias Mountains.

Limitations and future work

Extensions to this work could include investigating sampling design, examining the effects of DEM gridcell size on winter balance and resolving temporal variability. Our sampling design was chosen to extensively sample the ablation area and is likely too finely resolved along transects for many future mass balance surveys to replicate. An optimized sampling design minimizes uncertainty while reducing the number of measurements, known as a data efficiency threshold. For example, López-Moreno and others (2010) concluded that 200–400 observations are needed to obtain accurate and robust snow distribution models within a non-glacierized alpine basin ($6\,km^2$).

DEM gridcell size is known to significantly affect computed topographic parameters and the ability to resolve important hydrological features (e.g. drainage pathways) in the basin (Zhang and Montgomery, 1994; Garbrecht and Martz, 1994; Guo-an and others, 2001; López-Moreno and others, 2010), with implications for linear regressions that use these topographic parameters. Zhang and Montgomery (1994) found that a 10 m gridcell size is an optimal compromise between resolution and data volume in the context of very small basins (0.3–1.2 km^2). Further, the relationship between topographic parameters and WB data is not independent of DEM gridcell size. For example, Kienzle (2004) and López-Moreno and others (2010) found that a decrease in spatial resolution of the DEM results in a decrease in the importance of curvature and an increase in the importance of elevation. DEM accuracy and resolution therefore affect the exploration of physical controls on basin-scale winter balance. However, increasing DEM resolution would still not resolve meter-scale variations in snow depth that are created by microtopography of ice. For example, the lower part of Glacier 2 has surface features with whale-back structure (metre-scale wavelengths) that results in highly variability snow depth.

Inter-annual variability in winter balance is not considered in our study. While this limits our conclusions, a number of studies have found temporal stability in spatial patterns of snow distribution and that statistical models based on topographic parameters could be applied reliable between years (e.g. Grünewald and others, 2013). For example, Walmsley (2015) analysed more than 40 years of accumulation recorded on two Norwegian glaciers and found that snow accumulation is spatially heterogeneous yet exhibits robust temporal stability in its distribution.

CONCLUSION

We estimate winter balance (WB) at various scales for three glaciers (termed as Glacier 2, Glacier 4 and Glacier 13) in the St. Elias Mountains from direct snow depth and density sampling. Our objectives are to (1) critically examine methods of moving from direct snow depth and density measurements to estimating WB and to (2) identify sources of uncertainty, evaluate their magnitude and assess their combined contribution to uncertainty in WB.

We find that interpolating and extrapolating gridcell-averaged WB has a large effect on glacier-wide WB. On Glacier 4, glacier-wide WB is consistent between linear regression (LR) and simple kriging (SK) but both explain only a small portion of the observed variance. This highlights that relatively precise glacier-wide WBs may not necessarily be accurate estimates. On Glaciers 2 and 13, LR and SK are better able to estimate gridcell-averaged WBs but glacier-wide WBs differ considerably between the two interpolation methods

due to extrapolation into the accumulation area. Gridcell-averaged WB on Glacier 4 is highly variable, as indicated by shorter range distance, higher nugget value and lower explained variance of gridcell-estimated WB. Glaciers 2 and 13 have lower gridcell-averaged WB variability and elevation is the primary control of observed variation.

For our study glaciers, the glacier-wide WB uncertainty ranges from 0.03 m w.e (8%) to 0.15 m w.e (54%), depending primarily on the interpolation method. Uncertainty within the interpolation method is the largest source of glacier-wide WB uncertainty when compared to uncertainty in grid-scale WB values and density assignment method. Future studies could reduce WB uncertainty by increasing the spatial distribution of snow depth sampling rather than the number of measurements within a single gridcell along a transect. In our work, increased sampling within the accumulation area would better constrain WB data extrapolation and decrease uncertainty. Despite challenges in accurately estimating WB, our data are consistent with a regional-scale WB gradient for the continental side of the St. Elias Mountains.

AUTHOR CONTRIBUTION STATEMENT

AP organized data collection, performed all calculations and wrote most of the paper. GEF supported data collection, supervised the findings of this work and provided substantial edits to the paper. VR provided guidance with statistical methods and contributed to paper edits.

ACKNOWLEDGEMENTS

We thank the Kluane First Nation (KFN), Parks Canada and the Yukon Territorial Government for granting us permission to work in traditional KFN territory and Kluane National Park and Reserve. We are grateful for financial support provided by the Natural Sciences and Engineering Research Council of Canada, Simon Fraser University, the Northern Scientific Training Program and the Polar Continental Shelf Project. We kindly acknowledge Trans North Helicopter pilot Dion Parker, and the Arctic Institute of North America's Kluane Lake Research Station for facilitating field logistics. We are grateful to Alison Criscitiello and Coline Ariagno for all aspects of field assistance and Sarah Furney for data entry assistance. Thank you to Etienne Berthier for providing us with the SPIPT SPOT-5 DEM and for assistance with correcting two DEM sections. We are grateful to Derek Bingham and Michael Grosskopf for assistance with the statistics, including simple kriging. Anonymous reviewers, Luke Wonneck, Leif Anderson and Jeff Crompton all provided thoughtful and constructive comments on the manuscript.

REFERENCES

Anderton S, White S and Alvera B (2004) Evaluation of spatial variability in snow water equivalent for a high mountain catchment. *Hydrological Processes*, **18**(3), 435–453 (doi: 10.1002/hyp.1319)

Bagos PG and Adam M (2015) On the Covariance of Regression Coefficients. *Open Journal of Statistics*, **5**(07), 680 (doi: 10.4236/ojs.2015.57069)

Balk B and Elder K (2000) Combining binary decision tree and geostatistical methods to estimate snow distribution in a mountain watershed. *Water Resources Research*, **36**(1), 13–26 (doi: 10.1029/1999WR900251)

Barry RG (1992) *Mountain weather and climate*. Cambridge Univserity Press, 3rd edition

Beauont RT and Work RA (1963) Snow sampling results from three samplers. *International Association of Scientific Hydrology. Bulletin*, **8**(4), 74–78 (doi: 10.1080/02626666309493359)

Burnham KP and Anderson DR (2004) Multimodel Inference: Understanding AIC and BIC in Model Selection. *Sociological Methods & Research*, **33**(2), 261–304 (doi: 10.1177/0049124104268644)

Clark MP, Hendrikx J, Slater AG, Kavetski D, Anderson B, Cullen NJ, Kerr T, Örn Hreinsson E and Woods RA (2011) Representing spatial variability of snow water equivalent in hydrologic and land-surface models: A review. *Water Resources Research*, **47**(7) (doi: 10.1029/2011WR010745)

Clarke GK (2014) A short and somewhat personal history of Yukon glacier studies in the Twentieth Century. *Arctic*, **37**(1), 1–21

Clyde GD (1932) Circular No. 99-Utah Snow Sampler and Scales for Measuring Water Content of Snow. *UAES Circulars*, Paper 90

Cogley J, Hock R, Rasmussen L, Arendt A, Bauder A, Braithwaite R, Jansson P, Kaser G, Möller M, Nicholson L and others (2011) *Glossary of glacier mass balance and related terms*. UNESCO-IHP, Paris

Conger SM and McClung DM (2009) Comparison of density cutters for snow profile observations. *Journal of Glaciology*, **55**(189), 163–169

Crompton JW and Flowers GE (2016) Correlations of suspended sediment size with bedrock lithology and glacier dynamics. *Annals of Glaciology*, 1–9 (doi: 10.1017/aog.2016.6)

Cullen NJ, Anderson B, Sirguey P, Stumm D, Mackintosh A, Conway JP, Horgan HJ, Dadic R, Fitzsimons SJ and Lorrey A (2017) An 11-year record of mass balance of Brewster Glacier, New Zealand, determined using a geostatistical approach. *Journal of Glaciology*, **63**(238), 199–217 (doi: 10.1017/jog.2016.128)

523 Dadić R, Mott R, Lehning M and Burlando P (2010) Parameterization for wind-induced preferential
524 deposition of snow. *Journal of Geophysical Research: Earth Surface (2003–2012)*, **24**(14), 1994–2006 (doi:
525 10.1029/2009JF001261)

526 Danby RK, Hik DS, Slocombe DS and Williams A (2003) Science and the St. Elias: an evolving framework
527 for sustainability in North America's highest mountains. *The Geographical Journal*, **169**(3), 191–204 (doi:
528 10.1111/1475-4959.00084)

529 Davis JC and Sampson RJ (1986) *Statistics and data analysis in geology*. Wiley New York et al., 2nd edition

530 Deems JS and Painter TH (2006) Lidar measurement of snow depth: accuracy and error sources. In
531 *Proceedings of the International Snow Science Workshop*

532 Dixon D and Boon S (2012) Comparison of the SnowHydro snow sampler with existing snow tube designs.
533 *Hydrological Processes*, **26**(17), 2555–2562, ISSN 1099-1085 (doi: 10.1002/hyp.9317)

534 Egli L, Griessinger N and Jonas T (2011) Seasonal development of spatial snow-depth variability across dif-
535 ferent scales in the Swiss Alps. *Annals of Glaciology*, **52**(58), 216–222 (doi: 10.3189/172756411797252211)

536 Elder K, Dozier J and Michaelsen J (1991) Snow accumulation and distribution in an alpine watershed.
537 *Water Resources Research*, **27**(7), 1541–1552 (doi: 10.1029/91WR00506)

538 Elder K, Rosenthal W and Davis RE (1998) Estimating the spatial distribution of snow water equivalence
539 in a montane watershed. *Hydrological Processes*, **12**(1011), 1793–1808 (doi: 10.1002/(SICI)1099-
540 1085(199808/09)12:10/111793::AID-HYP6953.0.CO;2-K)

541 Erxleben J, Elder K and Davis R (2002) Comparison of spatial interpolation methods for estimating
542 snow distribution in the Colorado Rocky Mountains. *Hydrological Processes*, **16**(18), 3627–3649 (doi:
543 10.1002/hyp.1239)

544 Fames PE, Peterson N, Goodison B and Richards RP (1982) Metrication of Manual Snow Sampling
545 Equipment. In *Proceedings of the 50th Western Snow Conference*, 120–132

546 Fierz C, Armstrong RL, Durand Y, Etchevers P, Greene E, McClung DM, Nishimura K, Satyawali PK
547 and Sokratov SA (2009) *The international classification for seasonal snow on the ground*, volume 25.
548 UNESCO/IHP Paris

549 Garbrecht J and Martz L (1994) Grid size dependency of parameters extracted from digital elevation models.
550 *Computers & Geosciences*, **20**(1), 85–87, ISSN 0098-3004 (doi: 10.1016/0098-3004(94)90098-1)

Gerber F, Lehning M, Hoch SW and Mott R (2017) A close-ridge small-scale atmospheric flow field and its influence on snow accumulation. *Journal of Geophysical Research: Atmospheres*, n/a–n/a, ISSN 2169-8996 (doi: 10.1002/2016JD026258), 2016JD026258

Grabiec M, Puczko D, Budzik T and Gajek G (2011) Snow distribution patterns on Svalbard glaciers derived from radio-echo soundings. *Polish Polar Research*, **32**(4), 393–421 (doi: 10.2478/v10183-011-0026-4)

Gray DM and Male DH (1981) *Handbook of snow: principles, processes, management & use*. Pergamon Press, 1st edition

Grunewald T, Schirmer M, Mott R and Lehning M (2010) Spatial and temporal variability of snow depth and ablation rates in a small mountain catchment. *Cryosphere*, **4**(2), 215–225 (doi: 10.5194/tc-4-215-2010)

Grünewald T, Stötter J, Pomeroy J, Dadic R, Moreno Baños I, Marturià J, Spross M, Hopkinson C, Burlando P and Lehning M (2013) Statistical modelling of the snow depth distribution in open alpine terrain. *Hydrology and Earth System Sciences*, **17**(8), 3005–3021 (doi: 10.5194/hess-17-3005-2013)

Guo-an T, Yang-he H, Strobl J and Wang-qing L (2001) The impact of resolution on the accuracy of hydrologic data derived from DEMs. *Journal of Geographical Sciences*, **11**(4), 393–401, ISSN 1861-9568 (doi: 10.1007/BF02837966)

Gusmeroli A, Wolken GJ and Arendt AA (2014) Helicopter-borne radar imaging of snow cover on and around glaciers in Alaska. *Annals of Glaciology*, **55**(67), 78–88 (doi: 10.3189/2014AoG67A029)

Helbig N and van Herwijnen A (2017) Subgrid parameterization for snow depth over mountainous terrain from flat field snow depth. *Water Resources Research*, **53**(2), 1444–1456, ISSN 0043-1397 (doi: 10.1002/2016WR019872)

Hock R (2005) Glacier melt: a review of processes and their modelling. *Progress in Physical Geography*, **29**(3), 362–391 (doi: 10.1191/0309133305pp453ra)

Hock R and Jensen H (1999) Application of kriging interpolation for glacier mass balance computations. *Geografiska Annaler: Series A, Physical Geography*, **81**(4), 611–619 (doi: 10.1111/1468-0459.00089)

Kaser G, Fountain A, Jansson P and others (2002) *A manual for monitoring the mass balance of mountain glaciers*. IHP-VI- Technical documents in hydrology

Kienzle S (2004) The Effect of DEM Raster Resolution on First Order, Second Order and Compound Terrain Derivatives. *Transactions in GIS*, **8**(1), 83–111, ISSN 1467-9671 (doi: 10.1111/j.1467-9671.2004.00169.x)

Kohavi R and others (1995) A study of cross-validation and bootstrap for accuracy estimation and model selection. In *Proceedings of the Fourteenth International Joint Conference on Artificial Intelligence*, volume 14, 1137–1145

Lehning M, Völksch I, Gustafsson D, Nguyen TA, Stähli M and Zappa M (2006) ALPINE3D: a detailed model of mountain surface processes and its application to snow hydrology. *Hydrological Processes*, **20**(10), 2111–2128 (doi: 10.1002/hyp.6204)

Li J and Heap AD (2008) A review of spatial interpolation methods for environmental scientists. *Geoscience Australia*, Record 2008/23

Liston GE and Elder K (2006) A distributed snow-evolution modeling system (SnowModel). *Journal of Hydrometeorology*, **7**(6), 1259–1276 (doi: 10.1175/JHM548.1)

López-Moreno J, Latron J and Lehmann A (2010) Effects of sample and grid size on the accuracy and stability of regression-based snow interpolation methods. *Hydrological Processes*, **24**(14), 1914–1928, ISSN 1099-1085 (doi: 10.1002/hyp.7564)

López-Moreno J, Fassnacht S, Heath J, Musselman K, Revuelto J, Latron J, Morán-Tejeda E and Jonas T (2013) Small scale spatial variability of snow density and depth over complex alpine terrain: Implications for estimating snow water equivalent. *Advances in Water Resources*, **55**, 40–52 (doi: 10.1016/j.advwatres.2012.08.010)

López-Moreno JI, Fassnacht S, Beguería S and Latron J (2011) Variability of snow depth at the plot scale: implications for mean depth estimation and sampling strategies. *The Cryosphere*, **5**(3), 617–629 (doi: 10.5194/tc-5-617-2011)

MacDougall AH and Flowers GE (2011) Spatial and temporal transferability of a distributed energy-balance glacier melt model. *Journal of Climate*, **24**(5), 1480–1498 (doi: 10.1175/2010JCLI3821.1)

Machguth H, Eisen O, Paul F and Hoelzle M (2006) Strong spatial variability of snow accumulation observed with helicopter-borne GPR on two adjacent Alpine glaciers. *Geophysical Research Letters*, **33**(13), 1–5 (doi: 10.1029/2006GL026576)

Madigan D and Raftery AE (1994) Model Selection and Accounting for Model Uncertainty in Graphical Models Using Occam's Window. *Journal of the American Statistical Association*, **89**(428), 1535–1546, ISSN 01621459

Marshall HP, Koh G, Sturm M, Johnson J, Demuth M, Landry C, Deems J and Gleason J (2006) Spatial variability of the snowpack: Experiences with measurements at a wide range of length scales with several different high precision instruments. In *Proceedings International Snow Science Workshop*, 359–364

McGrath D, Sass L, O'Neel S, Arendt A, Wolken G, Gusmeroli A, Kienholz C and McNeil C (2015) End-of-winter snow depth variability on glaciers in Alaska. *Journal of Geophysical Research: Earth Surface*, **120**(8), 1530–1550 (doi: 10.1002/2015JF003539)

Metropolis N and Ulam S (1949) The Monte Carlo Method. *Journal of the American Statistical Association*, **44**(247), 335–341, ISSN 01621459

Molotch N, Colee M, Bales R and Dozier J (2005) Estimating the spatial distribution of snow water equivalent in an alpine basin using binary regression tree models: the impact of digital elevation data and independent variable selection. *Hydrological Processes*, **19**(7), 1459–1479 (doi: 10.1002/hyp.5586)

Mott R, Faure F, Lehning M, Löwe H, Hynek B, Michlmayer G, Prokop A and Schöner W (2008) Simulation of seasonal snow-cover distribution for glacierized sites on Sonnblick, Austria, with the Alpine3D model. *Annals of Glaciology*, **49**(1), 155–160 (doi: 10.3189/172756408787814924)

Musselman KN, Pomeroy JW, Essery RL and Leroux N (2015) Impact of windflow calculations on simulations of alpine snow accumulation, redistribution and ablation. *Hydrological Processes*, **29**(18), 3983–3999 (doi: 10.1002/hyp.10595)

Raftery AE, Madigan D and Hoeting JA (1997) Bayesian Model Averaging for Linear Regression Models. *Journal of the American Statistical Association*, **92**(437), 179–191 (doi: 10.1080/01621459.1997.10473615)

Réveillet M, Vincent C, Six D and Rabatel A (2016) Which empirical model is best suited to simulate glacier mass balances? *Journal of Glaciology*, **63**(237), 1–16 (doi: 10.1017/jog.2016.110)

Roustant O, Ginsbourger D and Deville Y (2012) DiceKriging, DiceOptim: Two R packages for the analysis of computer experiments by kriging-based metamodeling and optimization. *Journal of Statistical Software*, **21**, 1–55

Schneiderbauer S and Prokop A (2011) The atmospheric snow-transport model: SnowDrift3D. *Journal of Glaciology*, **57**(203), 526–542 (doi: 10.3189/002214311796905677)

Schuler TV, Crochet P, Hock R, Jackson M, Barstad I and Jóhannesson T (2008) Distribution of snow accumulation on the Svartisen ice cap, Norway, assessed by a model of orographic precipitation. *Hydrological Processes*, **22**(19), 3998–4008, ISSN 1099-1085 (doi: 10.1002/hyp.7073)

Shea C and Jamieson B (2010) Star: an efficient snow point-sampling method. *Annals of Glaciology*, **51**(54), 64–72 (doi: 10.3189/172756410791386463)

Sold L, Huss M, Hoelzle M, Andereggen H, Joerg PC and Zemp M (2013) Methodological approaches to infer end-of-winter snow distribution on alpine glaciers. *Journal of Glaciology*, **59**(218), 1047–1059 (doi: 10.3189/2013JoG13J015)

Tangborn WV, Krimmel RM and Meier MF (1975) A comparison of glacier mass balance by glaciological, hydrological and mapping methods, South Cascade Glacier, Washington. *International Association of Hydrological Sciences Publication*, **104**, 185–196

Taylor-Barge B (1969) *The summer climate of the St. Elias Mountain region*. Montreal: Arctic Institute of North America, Research Paper No. 53

Thibert E, Blanc R, Vincent C and Eckert N (2008) Glaciological and volumetric mass-balance measurements: error analysis over 51 years for Glacier de Sarennes, French Alps. *Journal of Glaciology*, **54**(186), 522–532

Trujillo E and Lehning M (2015) Theoretical analysis of errors when estimating snow distribution through point measurements. *The Cryosphere*, **9**(3), 1249–1264 (doi: 10.5194/tc-9-1249-2015)

Turcan J and Loijens H (1975) Accuracy of snow survey data and errors in snow sampler measurements. In *32nd Eastern Snow Conference*

Walmsley APU (2015) *Long-term observations of snow spatial distributions at Hellstugubreen and Gråsubreen, Norway*. Master's thesis

Wetlaufer K, Hendrikx J and Marshall L (2016) Spatial Heterogeneity of Snow Density and Its Influence on Snow Water Equivalence Estimates in a Large Mountainous Basin. *Hydrology*, **3**(3), 1–17 (doi: 10.3390/hydrology3010003)

Winstral A, Marks D and Gurney R (2013) Simulating wind-affected snow accumulations at catchment to basin scales. *Advances in Water Resources*, **55**, 64–79 (doi: 10.1016/j.advwatres.2012.08.011)

Winther J, Bruland O, Sand K, Killingtveit A and Marechal D (1998) Snow accumulation distribution on Spitsbergen, Svalbard, in 1997. *Polar Research*, **17**, 155–164

Woo MK and Marsh P (1978) Analysis of Error in the Determination of Snow Storage for Small High Arctic Basins. *Journal of Applied Meteorology*, **17**(10), 1537–1541

Wood WA (1948) Project "Snow Cornice": the establishment of the Seward Glacial research station. *Arctic*, **1**(2), 107–112

Work R, Stockwell H, Freeman T and Beaumont R (1965) *Accuracy of field snow surveys*. Cold Regions Research & Engineering Laboratory

Zhang W and Montgomery DR (1994) Digital elevation model grid size, landscape representation, and hydrologic simulations. *Water Resources Research*, **30**(4), 1019–1028 (doi: 10.1029/93WR03553)